

# Long-range adiabatic quantum state transfer through a linear array of quantum dots

CHEN Bing<sup>a,\*</sup>, FAN Wei<sup>a</sup>, XU Yan<sup>a,b,\*</sup>

<sup>a</sup>College of Science, Shandong University of Science and Technology, Qingdao 266510, China

<sup>b</sup>Centre for Quantum Technologies, National University of Singapore, 3 Science drive 2, Singapore 117543

---

## Abstract

We introduce an adiabatic long-range quantum communication proposal based on a quantum dot array. By adiabatically varying the external gate voltage applied on the system, the quantum information encoded in the electron can be transported from one end dot to another. We numerically solve the Schrödinger equation for a system with a given number of quantum dots. It is shown that this scheme is a simple and efficient protocol to coherently manipulate the population transfer under suitable gate pulses. The dependence of the energy gap and the transfer time on system parameters is analyzed and shown numerically. We also investigate the adiabatic passage in a more realistic system in the presence of inevitable fabrication imperfections. This method provides guidance for future realizations of adiabatic quantum state transfer in experiments.

**Keywords:** adiabatic passage, tight-binding model, quantum state transfer

**PACS:** 03.65.-w, 03.67.Hk, 73.23.Hk

---

## 1. Introduction

In quantum information science, quantum state transfer (QST), as the name suggests, refers to the transfer of an arbitrary quantum state  $\alpha|0\rangle + \beta|1\rangle$  from one qubit to another. There are two major mechanisms for QST in quantum mechanics. The first approach is usually characterized by preparing the quantum channel with an *always-on* interaction where QST is equivalent to the time evolution of the quantum state in the time-independent Hamiltonian [1, 2, 3]. However, these approaches require precise control of distance and timing. Any deviation may lead to significant errors. The other approach has paid much attention to adiabatic passage for coherent QST in time-evolving quantum systems, which is a powerful tool for manipulating a quantum system from an initial state to a target state. This method of population transfer has the important property of being robust against small variations of the Hamiltonian and the transport time, which is crucial experimentally since the system parameters are often hard to control. Recently, the adiabatic method has been

applied to a variety of physical systems to realize coherent QST. Among these, the typical scheme for coherently spatial population transfer has been independently proposed for neutral atoms in optical traps [4] and for electrons in quantum dot (QD) systems [5] via a dark state of the system, which is termed coherent tunneling via adiabatic passage (CTAP) following [5]. In such a scheme, the tunneling interaction between adjacent quantum units is dynamically tuned by changing either the distance or the height of the neighboring potential wells following a counterintuitive scheme, which is a solid-state analog of the well-known stimulated Raman adiabatic passage (STIRAP) protocol [6] of quantum optics. Since then, the CTAP technique has been proposed in a variety of physical systems for transporting single atoms [7, 8], spin states [9], electrons [10, 11] and Bose-Einstein condensates [12, 13, 14]. It has also been proposed as a crucial element in the scale up to large quantum processors [15, 16].

Recently, Ref. [17] presented a scheme to adiabatically transfer an electron from the left end to the right end of a three dot chain using the ground state of the system. This technique is a copy of the frequency chirping method [18, 19], which is used in quantum optics to transfer the population of a three-level atom of the Lambda configuration. The scheme [17] is pre-

---

\*Corresponding author

Email addresses: chenbingphys@gmail.com (CHEN Bing), x1y5@hotmail.com (XU Yan)

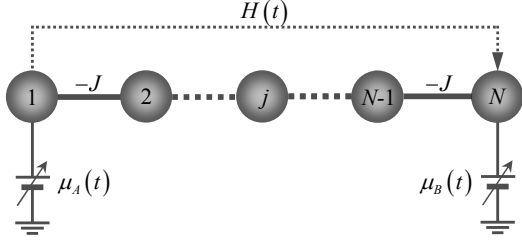


Figure 1: Schematic illustrations of adiabatic QST in a multi-dot array. The system is controlled by gate voltages,  $\mu_\alpha(t)$  ( $\alpha = A, B$ ). By adiabatically varying the gate voltages, one can achieve long-range QST from the left end to the right QD of the proposal.

sented as an alternative to a well known transfer scheme (CTAP) [5]. However, different from the CTAP process, the protocol in Ref. [17] considers a three QD array with an *always-on* interaction that can be manipulated by the external gate voltage applied on the two external dots (sender and receiver). Through maintaining the system in the ground state, it shows that it is a high-fidelity process for a proper choice of system parameters and also robust against experimental parameter variations. In this paper we will consider the passage through the  $N$ -site coupled QDs array (tight-binding model), which is schematically illustrated in Fig. 1. Gates applied on the two end dots control the on-site energy of each dot. In particular, the nearest-neighbor hopping amplitudes are set to be uniform. We first investigate the effect of system parameters on the minimum energy gap between the ground state and the first excited state. Taking a 5-dot structure as an example, we show that the electron can be robustly transported from one end of the chain to the other by slowly varying the gate voltages. This structure is easy to extend to an arbitrary number of sites.

The paper is organized as follows. In Sec. II the model is setup and we describe the adiabatic transfer of an electron between QDs. In Sec. III we show numerical results that substantiate the analytical results. The last section is the summary and discussion of the paper.

## 2. Model setup

We introduce a simple tight-binding chain with uniform nearest-neighbor hopping integral  $-J$  as a quantum data bus for long-range quantum transport, see Fig. 1. The sender (Alice) and the receiver (Bob) can only control the external gate voltages  $\mu_\alpha(t)$  ( $\alpha = A, B$ ), which are applied on the two end QDs. In this proposal, the quantum information  $\cos \theta |\uparrow\rangle + \sin \theta |\downarrow\rangle$  encoded in the polarization of the electron can be transported from

Alice to Bob. In this scheme the spin state of the electron is a conserved quantity for the Hamiltonian of the medium, so the spin state cannot be influenced during the propagation. For simplicity, we will disregard the electron's spin degrees of freedom in the following discussion and just illustrate the principles of QST.

Accounting only for the occupation of the lowest single-particle state of each dot, the system is described by an  $N$ -site tight-binding chain. The Hamiltonian can be written as

$$\begin{aligned}\mathcal{H}(t) &= \mathcal{H}_M + \mathcal{H}_C, \\ \mathcal{H}_M &= -J \sum_{j=1}^{N-1} (a_j^\dagger a_{j+1} + \text{h.c.}), \\ \mathcal{H}_C &= \mu_A(t) a_1^\dagger a_1 + \mu_B(t) a_N^\dagger a_N,\end{aligned}\quad (1)$$

where  $a_j^\dagger(a_j)$  denotes the spinless fermion creation (annihilation) operator at the  $j$ -th quantum site.  $-J$  ( $J > 0$ ) is the coupling constant, which accounts for the hopping of the electron between dots  $j$  and  $j+1$ . The on-site energies  $\mu_A(t)$  and  $\mu_B(t)$  are modulated in Gaussian pulses to realize the adiabatic transfer, according to [shown in Fig. 2(a)]

$$\mu_A(t) = -\mu_{A,\max} \exp[-\alpha^2 t^2 / 2], \quad (2a)$$

$$\mu_B(t) = -\mu_{B,\max} \exp[-\alpha^2 (t - \tau)^2 / 2], \quad (2b)$$

where  $\tau$  and  $\alpha$  are the total adiabatic evolution time and standard deviation of the control pulse. For simplicity we set the two peak values to be equal, i.e.,  $\mu_{A,\max} = \mu_{B,\max} = \mu_0$  ( $\mu > 0$ ), in the discussion that follows and choose  $\mu_0 \gg J$ .

In this proposal, we will concentrate on the single-particle problem and use the ground state  $|\psi_g(t)\rangle$  of the Hamiltonian  $\mathcal{H}(t)$  to induce a population transfer from state  $|1\rangle$  to  $|N\rangle$ . Starting from  $t = 0$ , we have  $\mu_A(0) = -\mu_0$  and  $\mu_B(0) \approx 0$ . The Hamiltonian at  $t = 0$  reads

$$\mathcal{H}(t=0) = -\mu_0 a_1^\dagger a_1 - J \sum_{j=1}^{N-1} (a_j^\dagger a_{j+1} + \text{h.c.}). \quad (3)$$

The ground state of Eq. (3) is a bound state, which can be obtained via the Bethe ansatz method. A straightforward calculation shows that

$$|\psi_g(t=0)\rangle = \sqrt{1 - \zeta^2} \sum_{j=1}^N \zeta^{j-1} |j\rangle, \quad (4)$$

where  $\zeta = J/\mu_0$ . By choosing a sufficiently large value of  $\mu_0$ , the ground state  $|\psi_g(0)\rangle$  can be reduced to  $|\psi_g(0)\rangle \approx |1\rangle = a_1^\dagger |0\rangle$ . To illustrate with an example,

the probability of  $|1\rangle$  in  $|\psi_g(t=0)\rangle$  can achieve 99.75% when the peak voltage is set to be  $\mu_0/J = 20$ .

With the same reasoning, in the time limit  $t = \tau$ , the parameter  $\mu_A(t)$  goes to zero and  $\mu_B(t)$  goes to  $-\mu_0$ . Due to the reflection symmetry (relabelling sites from right to left) of the system, we can see that

$$|\psi_g(t=\tau)\rangle = \sqrt{1-\zeta^2} \sum_{j=1}^N \zeta^{N-j} |j\rangle. \quad (5)$$

One can see that the ground state of Eq. (1) evolves to be  $|\psi_g(t=\tau)\rangle \approx |N\rangle$ . Preparing the system in state  $|\Psi(t=0)\rangle = |1\rangle$  and adiabatically changing  $\mu_A(t)$  and  $\mu_B(t)$ , one can see that the system will end up in  $|N\rangle$

$$|\Psi(t=0)\rangle = |1\rangle \rightarrow |\Psi(t=\tau)\rangle = |N\rangle. \quad (6)$$

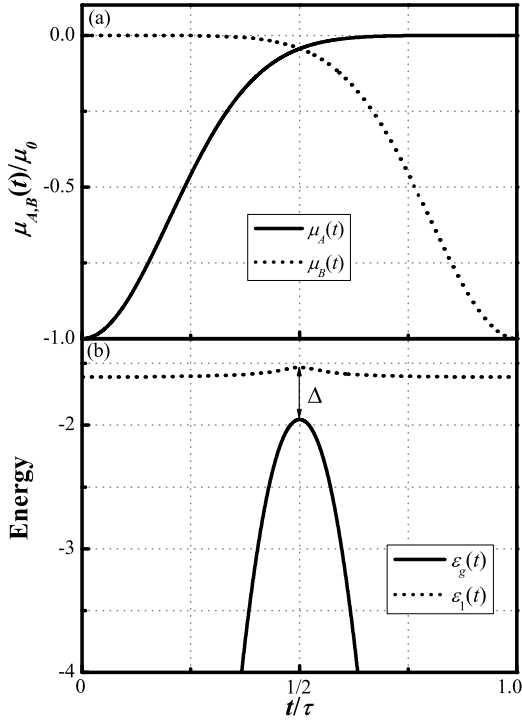


Figure 2: (a) Gate voltages (in units of  $\mu_0$ ) as a function of time (in units of  $\tau$ ) described in Eq. (2).  $\mu_A(t)$  is the solid line and  $\mu_B(t)$  is the dashed line. (b) The instantaneous eigenenergy of the lowest two states  $\psi_1$  and  $\psi_g$  through the gate pulse shown in (a) for the values of  $\mu_0 = 20$ ,  $J = 1.0$ , and  $\alpha = 5/\tau$  in an  $N = 5$  structure. The gap is minimum at  $t = \tau/2$ ,  $\Delta = \epsilon_1(\tau/2) - \epsilon_g(\tau/2)$ .

The analysis above is based on the assumption that the adiabaticity is satisfied. The crucial requirement for adiabatic evolution is

$$|\epsilon_g(t) - \epsilon_1(t)| \gg |\dot{\psi}_g(t)| |\psi_1(t)|, \quad (7)$$

which greatly suppresses the quantum transition from the ground state  $|\psi_g(t)\rangle$  to the first-excited state  $|\psi_1(t)\rangle$ . Firstly, one must make sure that no level crossings occur, i.e.,  $\epsilon_g(t) - \epsilon_1(t) < 0$ . To evaluate instantaneous eigenvalues of the Hamiltonian is generally only possible numerically. In Fig. 2(b) we present the results showing the eigenenergy gap between the instantaneous first-excited state and ground state undergoing evolution due to modulation of the gate voltage according to the pulses given in Eq. (2) for  $\mu_0 = 20$ ,  $J = 1.0$  and  $\alpha = 5/\tau$ . The eigenvalues shown in this figure exhibit pronounced avoided crossing and approach nonzero minimum  $\Delta = \epsilon_1(\tau/2) - \epsilon_g(\tau/2)$  at  $t = \tau/2$ . This minimum energy gap plays a significant role in the transfer, because the total evolution time  $\tau$  should be large compared to  $1/\Delta$ . In this scheme, the energy gap  $\Delta$  depends both on the number of QDs and gate voltages. To study the relationship between the total evolution time  $\tau$  and system parameters is one of the important contributions of this paper.

Fig. 3 shows the effect four factors have on the energy gap  $\Delta$ . In Fig. 3(a), for a given  $\alpha = 5/\tau$  and  $J = 1.0$ , we plot the energy gap  $\Delta$  as a function of  $N^{-2}$  for  $\mu_0 = 16, 20$ , and  $24$ . The numerical results indicate that the gap  $\Delta \sim J^2/(\mu_0 N^2)$ , which implies that the adiabatic transfer time of QST grows quadratically with the spatial separation of the two end states because the minimum gap plays an opposite role for the adiabatic QST. The other thing is that  $\Delta$  is also determined by the dimensionless parameter  $\alpha$ . As an example, Fig. 3(b) shows the numerically computed behavior of  $\Delta$  as a function of  $\alpha$  with  $N = 5$  and  $\mu_0/J = 20$ . From Fig. 3(b) we see that the gap becomes larger as  $\alpha$  increases and then tends to be a constant 0.732, which is the gap of tight-binding chain ( $N = 5$ ) without any on-site energy. The reason is that the bigger  $\alpha\tau$  is, the smaller the overlap amplitude of the two pulses, i.e.,  $\exp(-\alpha^2\tau^2/8) \rightarrow 0$ . The energy gap  $\Delta$  of  $\mathcal{H}(\tau/2)$  then approaches the maximum value  $2J[\cos \pi/(N+1) - \cos 2\pi/(N+1)]$ .

### 3. Numerical Examples

In this section let us firstly review the transfer process of this protocol. At  $t = 0$  we initialize the device so that the electron occupies site-1, i.e., the total initial state is  $|\Psi(0)\rangle = |1\rangle$ , and slowly apply gate pulses, which results in robust transport of the electron from one end of the chain to the other. The consequent time evolution of the state is given by the Schrödinger equation (assuming  $\hbar = 1$ )

$$i \frac{d}{dt} |\Psi(t)\rangle = \mathcal{H}(t) |\Psi(t)\rangle. \quad (8)$$

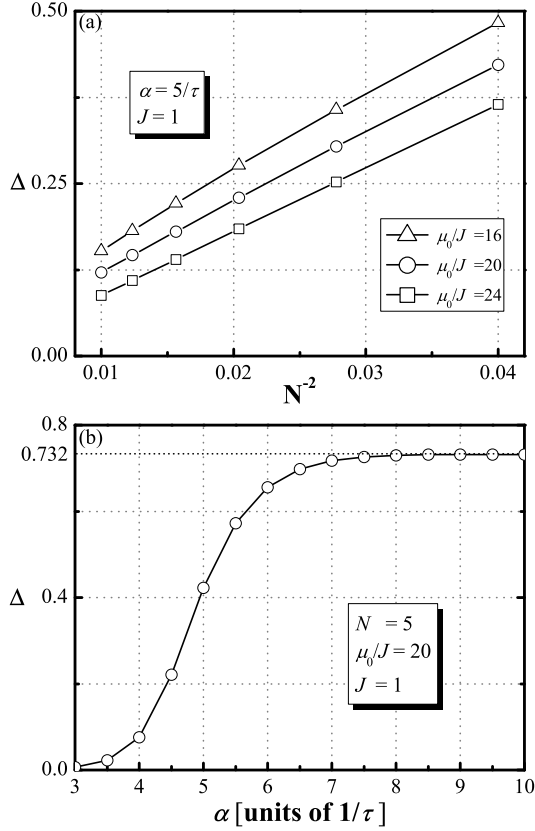


Figure 3: Effect the system parameters have on the energy difference. (a) The gap  $\Delta$  obtained using a numerical method for the systems  $N = 5, 6, 7, 8, 9$ , and  $10$ , with  $\mu_0 = 16, 20, 24$  and  $J = 1.0$  are plotted. It indicates that  $\Delta \sim J^2 / (\mu_0 N^2)$ . (b) The gap  $\Delta$  as a function of  $\alpha$ . It shows the increase of the gap with increasing  $\alpha$ .

The time evolution creates a coherent superposition:

$$|\Psi(t)\rangle = \sum_{j=1}^N c_j(t) |j\rangle, \quad (9)$$

where  $c_j(t)$  denotes the time-dependent probability amplitude for the electron to be in the  $j$ -th QD that obeys the normalization condition  $\sum_{j=1}^N |c_j(t)|^2 = 1$ . At time  $\tau$  the fidelity of the initial state transferring to the dot- $N$  is defined as

$$F(\tau) = |\langle N | \Psi(\tau) \rangle|^2 = |c_N(\tau)|^2. \quad (10)$$

A feasible proposal should be able to perform efficient high-fidelity QST in the shortest possible time. In order to provide the most economical choice of parameters for reaching high transfer efficiency, we used standard numerical methods to integrate the Schrödinger equation for probability amplitudes. Because the

scheme relies on maintaining adiabatic conditions, we examine the effect of system parameters on the target state population.

We show in Fig. 4 the probabilities as a function of time for different values of  $\alpha$  where we take a 5-dot structure for example. The time behavior of  $\mu_A(t)$  and  $\mu_B(t)$  follow Gaussian functions with  $\mu_0/J = 20$  [see Fig. 2(a)] and have been performed in a finite time.

For the  $\alpha = 4/\tau$  case with  $\tau = 500$ , which departs from the adiabatic limit, we find the result in Fig. 4(a). Here the population transferred to the target state is only about 11%. The reason is that the population is excited to the upper energy states through nonadiabaticity. It is necessary to point out that if one enlarged  $\tau$  extremely in this case, adiabaticity would be fulfilled, which would result in high transfer fidelity.

On the other hand, as shown in Fig. 3, enlarging  $\alpha$  can increase the level spacing between the first excited state and the ground state and hence cause the adiabaticity of the system to become better. In Fig. 4(b) we show the population evolution taking  $\alpha = 5/\tau$  as an example and the populations of the states  $|1\rangle$  and  $|N\rangle$  are exchanged with a fidelity of 99.5%.

The choice of pulse modulation is therefore important with the maximum transfer speed ultimately controlled by the adiabatic criteria for the transfer. To see the emergence of the adiabatic limit, we plot in Fig. 4(c) the transfer fidelity as a function of the adiabaticity parameter  $\alpha$ . One can see that as  $\alpha$  increases there is an exponential appearance of the adiabaticity in the ideal limit. That means the smaller the overlapping of two pulses is, the more ideal adiabatic transfer takes place. This result is extendible to an arbitrary number of QDs. In the discussion that follows, we choose  $\alpha = 5/\tau$ .

In section II, we showed that the energy gap  $\Delta$  also depends on the system parameters, such as the number of QDs  $N$  and coupling strength  $J$ . In order to quantitatively determine the time needed to achieve high fidelity QST, we solve the Schrödinger equation for constants  $\mu_0 = 20$ ,  $J = 1.0$ . In Fig. 5 we present results showing  $\tau$  as a function of the QDs number  $N$ . The quadratic curve fitting shows that the minimum possible transfer times are proportional to  $N^2$ , giving a high-fidelity transfer of  $|c_N(\tau)|^2 \geq 0.995$ . On the other hand, the energy gap  $\Delta$  decreases when the peak value rises [see Fig. 3(a)]. Consequently, the time scale  $\tau$  is proportional to and of the order of  $\mu_0/J^2$  for a given  $N$ . To sum up the above discussion, in practice the minimum possible transfer timescale of this adiabatic passage will be of the same order as  $N^2\mu_0/J^2$ .

For a long enough evolution time  $\tau$ , the maximum fidelity of this scheme depends on the contrast ratio be-

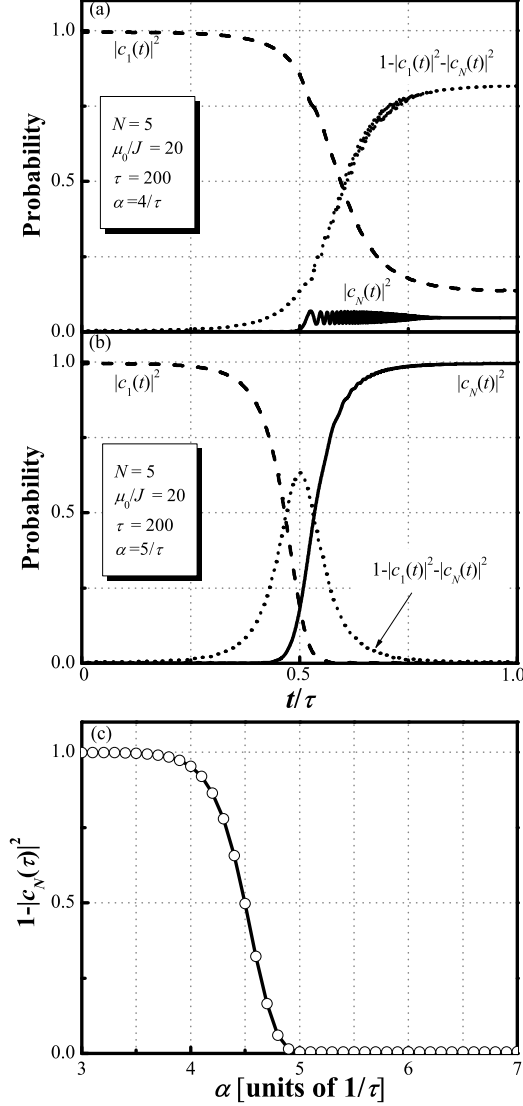


Figure 4: Probability of finding a single electron in basis states in the ground state as a function of time for the values of  $N = 5$ ,  $J = 1.0$ ,  $\mu_0 = 20$ ,  $\tau = 500$  and (a)  $\alpha = 4/\tau$ , (b)  $\alpha = 5/\tau$ . (c) Transfer fidelity  $|c_N(t)|^2$  as a function of parameter  $\alpha$ . As  $\alpha$  is increased it is more able to obtain high fidelity transfer. A smaller  $\alpha$  introduces a population of excited states and the transfer is no longer complete.

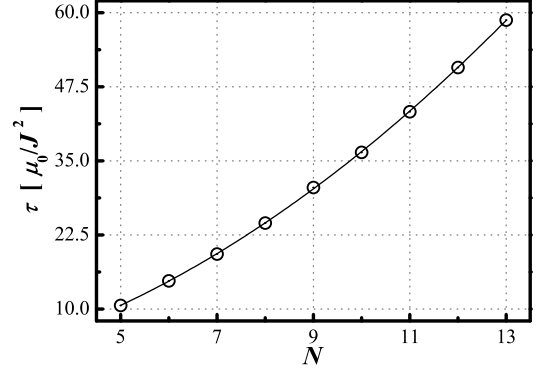


Figure 5: Total evolution time  $\tau$  (in units of  $\mu_0/J^2$ ) as  $N$  is increased under the condition that  $|c_N(\tau)|^2 \geq 0.995$ . As  $N$  is increased the energy gap is decreased, resulting in longer evolution time across the array. The solid line is the quadratic curve fitting, which indicates that the evolution time grows quadratically with the number of QDs.

tween peak values  $\mu_{\kappa, \max}$  ( $\kappa = A, B$ ) and coupling constants  $J$ . The reason is that small peak values improve adiabaticity, but lead to a low fidelity because the initial and final energy eigenstates are not the desired states  $|1\rangle$  and  $|N\rangle$ , respectively.

To determine the parameter range of  $\mu_{\kappa, \max}$  ( $\kappa = A, B$ ) needed to achieve high fidelity transfer, we numerically integrate the density matrix equations of motion, with varying peak values  $\mu_{A, \max}/J$  and  $\mu_{B, \max}/J$  from 10 to 25. Fig. 6 shows the transfer fidelity  $|c_N(\tau)|^2$  plots as a function of  $\mu_{A, \max}/J$  and  $\mu_{B, \max}/J$  for  $\tau = 1000$  and  $\alpha = 5/\tau$  in a 5-dot system. The fidelity approaches unity as  $\mu_{A, \max}$  and  $\mu_{B, \max}$  increase. The figure is nearly symmetric with respect to the line  $\mu_{A, \max} = \mu_{B, \max}$ . Fig. 6(a) is taken from Fig. 6(b) by slicing through the diagonal gray line. We can see that to realize near-perfect fidelity transfer ( $|c_N(\tau)|^2 \geq 0.995$ ) one has to use peak values satisfying  $\mu_{\kappa, \max} \geq 20J$  ( $\kappa = A, B$ ).

The other advantage of this scheme is defect tolerance of the system parameters. We now assume that the tunnel coupling has a random but constant offset  $\delta\epsilon_j$ , i.e.  $J_j = J(1 - \delta\epsilon_j)$ , where  $\epsilon_j$  is drawn from the standard uniform distribution on the open interval  $(0, 1)$  and all  $\epsilon_j$  are completely uncorrelated for all sites along the chain. We show some examples in Fig. 7 for QST in the chain of  $N = 5$  with maximum coupling offset bias  $\delta = 0.1, 0.2$ , and  $0.3$ . It shows that weak fluctuations (up to  $\delta = 0.2$ ) in the coupling strengths do not deteriorate the performance of our scheme. For  $\delta = 0.3$  we can see that arbitrarily perfect transfer remains possible except for some rare realizations of  $0.3\epsilon$ . To realize high-fidelity QST transfer, the price for unprecise couplings is thus a longer transmission time.



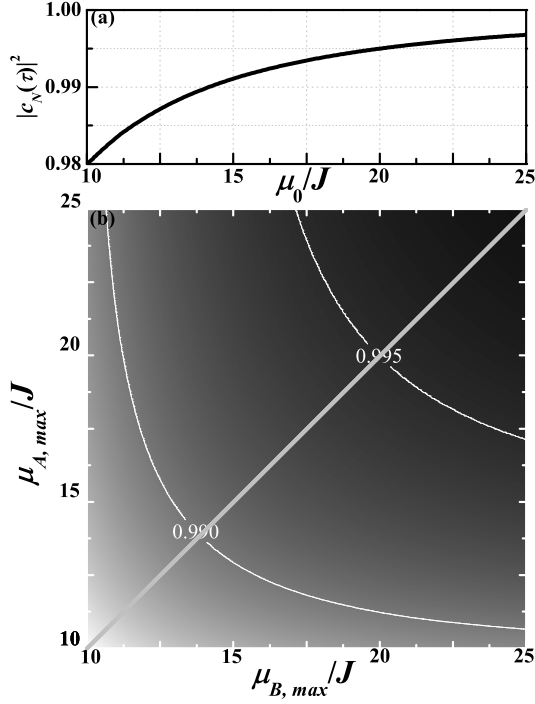


Figure 6: (Color online) Plot of the transfer fidelity  $|c_N(\tau)|^2$  as a function of peak values (in units of  $J$ ). (a)  $\mu_{A,max} = \mu_{B,max} = \mu_0$  varies from  $10J$  to  $25J$ ; (b)  $\mu_{A,max}$  and  $\mu_{B,max}$  vary from  $10J$  to  $25J$  respectively. The contour lines, labeled with the corresponding values of  $|c_N(\tau)|^2$ , display the gradual increase of transfer fidelity as  $\mu_{A,max}/J$  and  $\mu_{B,max}/J$  grow. The fidelity is close to one ( $|c_N(\tau)|^2 \geq 0.995$ ) when two peak values are achieved for  $\mu_{k,max} \geq 20J$  ( $k = A, B$ ).

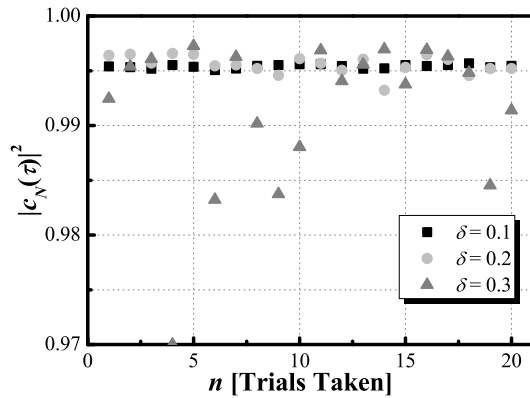


Figure 7: (Color online) The transfer fidelity  $|c_N(\tau)|^2$  for a tight-binding chain of length  $N = 5$  with  $\mu_{A,max} = \mu_{B,max} = 20J$ ,  $\tau = 500$  and  $\alpha = 5/\tau$ . The coupling strengths are chosen randomly from the interval  $[(1 - \delta)J, J]$  for  $\delta = 0.1$  (Square),  $\delta = 0.2$  (Circle) and  $\delta = 0.3$  (Triangle). The number of random samples is 20.

#### 4. Summary

We have introduced a robust and coherent method of long-range coherent QST through a tight-binding chain by adiabatic passage. This scheme is realized by modulation of gate voltages applied on the two end QDs. Under suitable gate pulses, the electron can be transported from one end of the chain to the other, carrying along with it the quantum information encoded in its spin. Different from the CTAPn Scheme [20], our method is to induce population transfer through the tight-binding chain by maintaining the system in its ground state and this is more operable in experiments. We have studied the adiabatic QST through the system by theoretical analysis and numerical simulations of the ground state evolution of the tight-binding model. The result shows that it is an efficient high-fidelity process ( $\geq 99.5\%$ ) for a proper choice of standard deviation  $\alpha \geq 5/\tau$  and peak values  $\mu_0 \geq 20$  of gate voltages. For an increasing number of dots, we found that the evolution time scale is  $\tau \sim N^2 \mu_0 / J^2$ . We also consider the QST along the quantum chain if their coupling is changed by some random amount. We further find that weak fluctuations in the coupling strength still allow high fidelity QST.

#### Acknowledgements

We acknowledge the support of the NSF of China (Grant No.10847150 and No.11105086), the Shandong Provincial Natural Science Foundation (Grant No. ZR2009AM026 and BS2011DX029), and the basic scientific research project of Qingdao (Grant No.11-2-4-4-(6)-jch). Y. X. also thanks the Basic Scientific Research Business Expenses of the Central University and Open Project of Key Laboratory for Magnetism and Magnetic Materials of the Ministry of Education, Lanzhou University (Grant No. LZUMMM2011001) for financial support.

#### References

- [1] Bose S. Quantum communication through an unmodulated spin chain. *Phys Rev Lett*, 2003, **91**(20): 207901
- [2] Song Z, Sun C P. Quantum information storage and state transfer based on spin systems. *Low Temperature Physics*, 2005 **31**(8): 686
- [3] Christandl M, Datta N, Ekert A, et al. Perfect State Transfer in Quantum Spin Networks. *Phys Rev Lett*, 2004, **92**(18): 187902
- [4] Eckert K, Lewenstein M, Corbal R, et al. Three-level atom optics via the tunneling interaction. *Phys Rev A*, 2004, **70**(2): 023606
- [5] Greentree A D, Cole J H, Hamilton A R, et al. Coherent electronic transfer in quantum dot systems using adiabatic passage. *Phys Rev B*, 2004, **70**(23): 235317

- [6] Vitanov N V, Halfmann T, Shore B W, et al. Laser-induced population transfer by adiabatic passage techniques. *Annu Rev Phys Chem*, 2001, **52**(1):763-809
- [7] Eckert K, Mompert J, Corbalan R, et al. Three level atom optics in dipole traps and waveguides. *Opt Commun*, 2006, **264**(2): 264-270
- [8] Opatrny T, Das K K. Conditions for vanishing central-well population in triple-well adiabatic transport. *Phys Rev A*, 2009, **79**(1): 012113
- [9] Ohshima T, Ekert A, Oi D K L, et al. Robust state transfer and rotation through a spin chain via dark passage. e-print arXiv:quant-ph/0702019.
- [10] Zhang P, Xue Q K, Zhao X G, et al. Generation of spatially separated spin entanglement in a triple-quantum-dot system. *Phys Rev A*, 2004, **69**(4): 042307
- [11] Fabian J, Hohenester U. Entanglement distillation by adiabatic passage in coupled quantum dots. *Phys Rev B*, 2005, **72**(20): 201304(R)
- [12] Graefe E M, Korsch H J, Witthaut D. Mean-field dynamics of a Bose-Einstein condensate in a time-dependent triple-well trap: Nonlinear eigenstates, Landau-Zener models, and stimulated Raman adiabatic passage. *Phys Rev A*, 2006, **73**(): 013617
- [13] Rab M, Cole J H, Parker N G, et al. Spatial coherent transport of interacting dilute Bose gases. *Phys Rev A*, 2008, **77**(6): 061602(R)
- [14] Nesterenko V O, Nikonov A N, de Souza Cruz F F, et al. STIRAP transport of Bose-Einstein condensate in triple-well trap. *Laser Phys*, 2009, **19**(4): 616-624
- [15] Hollenberg L C L, Greentree A D, Fowler A G, et al. Two-dimensional architectures for donor-based quantum computing. *Phys Rev B*, 2006, **74**(4): 045311
- [16] Greentree A D, Devitt S J, Hollenberg L C L. Quantum-information transport to multiple receivers. *Phys Rev A*, 2006, **73**(3): 032319
- [17] Chen B, Fan W, Xu Y. Adiabatic quantum state transfer in a nonuniform triple-quantum-dot system. *Phys Rev A*, 2011, **83**(1): 014301
- [18] Cheng J, Zhou J Y. Ultrafast population transfer in three-level  $\Lambda$  systems driven by few-cycle laser pulses. *Phys Rev A*, 2001 **64**(6): 065402
- [19] Goswami D. Optical pulse shaping approaches to coherent control. *Phys Rep*, 2003, **374**(6): 385-481
- [20] Hollenberg L C L, Greentree A D, Fowler A G, et al. Two-dimensional architectures for donor-based quantum computing. *Phys Rev B*, 2006, **74**(4): 045311